

# Relevance of the eigenstate thermalization hypothesis for thermal relaxation

Abdellah Khodja,<sup>1,\*</sup> Robin Steinigeweg,<sup>2,†</sup> and Jochen Gemmer<sup>1,‡</sup>

<sup>1</sup>*Department of Physics, University of Osnabrück, D-49069 Osnabrück, Germany*

<sup>2</sup>*Institute for Theoretical Physics, Technical University Braunschweig, D-38106 Braunschweig, Germany*

(Dated: July 24, 2018)

We study the validity of the eigenstate thermalization hypothesis (ETH) and its role for the occurrence of initial-state independent (ISI) equilibration in closed quantum many-body systems. Using the concept of dynamical typicality, we present an extensive numerical analysis of energy exchange in integrable and nonintegrable spin-1/2 systems of large size outside the range of exact diagonalization. In case of nonintegrable systems, our finite-size scaling shows that the ETH becomes valid in the thermodynamic limit and can serve as the underlying mechanism for ISI equilibration. In case of integrable systems, however, indication of ISI equilibration has been observed despite the violation of the ETH. We establish a connection between this observation and the need of choosing a proper parameter within the ETH.

PACS numbers: 05.30.-d, 75.10.Jm, 03.65.Yz, 05.45.Pq

## I. INTRODUCTION

Due to experiments in ultracold atomic gases [1–5], the question of thermalization in closed quantum systems has experienced an upsurge of interest in recent years. It is, however, a paradigm of standard thermodynamical processes that the final equilibrium state is generally independent of the details of the initial state. But this general initial-state independence (ISI) is challenging to proof from an underlying theory such as quantum mechanics. While for local density matrices of subsystems the issue of necessary and sufficient conditions for ISI is subtle [6, 7], for expectation values of observables a widely accepted *sufficient* condition for ISI is the validity of the eigenstate thermalization hypothesis (ETH) [8–10]. It claims that the expectation values of a given observable  $A$  should be similar for energy eigenstates  $|n\rangle$  if the energy eigenvalues  $E_n$  are close to each other, i.e.,  $\langle n|A|n\rangle \approx \langle n'|A|n'\rangle$  if  $E_n \approx E_{n'}$ . The relation to ISI equilibration can be seen from considering the dynamics

$$a(t) := \text{Tr}\{\rho(t) A\} = \sum_{nm} \rho_{nm} A_{mn} e^{i(E_m - E_n)t} \quad (1)$$

with  $A_{mn} = \langle m|A|n\rangle$  and averaging over sufficiently long times. Given that there are no degeneracies [11], this averaging yields

$$\bar{a} \approx \sum_n \rho_{nn} A_{nn}. \quad (2)$$

If, as the ETH claims, all  $A_{nn}$  from an energy region around  $E$  are similar, i.e.,  $A_{nn} \approx A(E)$ , then obviously  $\bar{a} \approx A(E)$  regardless of the initial state  $\rho(0)$ , as long as it is also restricted to the same energy region. Hence, if various  $a(t)$  from an energy shell equilibrate at all (for

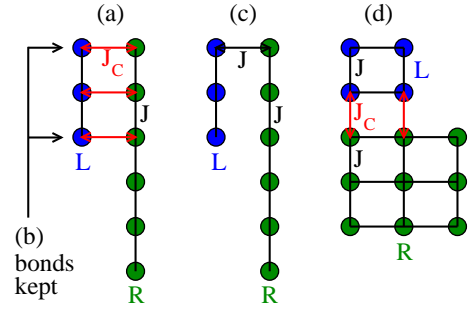


FIG. 1: (color online) Schematic representation of the systems for the study of energy exchange between a “left” (L) and “right” (R) part.

conditions on that see Refs. [7, 11]), they must do so at the same value  $A(E)$ , i.e., ISI applies.

Much less clear is whether or not the validity of the ETH is also a *physically necessary* condition for ISI in the sense that no *relevant* set of states can exhibit ISI without the ETH being fulfilled. (It is surely necessary if one requires that all states exhibit ISI.) Equation (2) allows for mathematically constructing different initial states with the same  $\bar{a}$  even in cases where the ETH does not apply (see, e.g., Refs. [12, 13]). Thus, the ETH may not be a physically necessary condition. However, the ETH has numerically been found to be fulfilled for a variety of systems and observables, and it is commonly expected that the ETH applies to few-body observables in nonintegrable quantum systems [8, 9, 16, 17]. But this expectation is still lacking a rigorous proof. Therefore, the crucial question is: Is the ETH the “force that drives” physical equilibration?

In the present paper, we consider this question by two different numerical approaches: i) We study the ETH concerning energy exchange for a variety of coupled subsystems. From the second law, ISI equilibration is strongly expected for each setting. ii) We investigate equilibration dynamics in systems for which the ETH is

\*Electronic address: akhodja@uos.de

†Electronic address: r.steinigeweg@tu-bs.de

‡Electronic address: jgemmer@uos.de

clearly violated. In both approaches, we apply the concept of dynamical typicality [18–22] and provide a careful finite-size scaling since, for any finite system, the ETH is never strictly fulfilled (i.e.,  $A_{nn} \neq A(E)$  except for trivial cases) [21, 23–25]. Our study in i) unveils that the ETH is fulfilled for energy exchange in nonintegrable systems and particularly approaches the thermodynamic limit according to a power-law dependence on the effective Hilbert-space dimension. Our investigations in ii) are different from other approaches based on quantum quenches [16, 26–30] or a period of time-dependent driving [31]. Still, we use pure initial states. But we prepare initial states with the property that the observable of interest deviates largely from its equilibrated value, while these states are still restricted to an energy shell. We consider this subclass of all possible initial states to be generic for equilibration experiments. As a main result, we observe ISI relaxation of energy exchange in an integrable system where the ETH clearly breaks down. In this way, we unveil the need of choosing a proper ETH-violation parameter.

This paper is structured as follows: In the next Sec. II we introduce the numerical method used as well as the models and observable studied. Then we summarize and discuss in Sec. III our results on the ETH and ISI equilibration in nonintegrable systems. The following Sec. III is devoted to the relationship between the ETH and ISI equilibration for the specific case of integrable systems and the above mentioned “observable-displaced” initial states. In the last Sec. V we summarize and draw conclusions.

## II. METHOD, MODELS, AND OBSERVABLE

Convenient parameters to quantify the ETH w.r.t. a given Hamiltonian  $H$  and observable  $A$  are

$$\bar{A} = \sum_{n=1}^d p_n A_{nn}, \quad \Sigma^2 = \sum_{n=1}^d p_n A_{nn}^2 - \bar{A}^2, \quad (3)$$

where  $A_{nn}$  are diagonal matrix elements w.r.t. the Hamiltonian eigenstates  $|n\rangle$  with eigenvalues  $E_n$ ,  $p_n \propto e^{-(E_n - \bar{E})^2/2\sigma^2}$  is a probability distribution centered at  $\bar{E}$ , and  $d$  is the Hilbert-space dimension. The quantities  $\bar{A}(\bar{E}, \sigma)$  and  $\Sigma(\bar{E}, \sigma)$  are obviously functions of  $\bar{E}$  and an energy width  $\sigma$ . Routinely, the ETH is said to be fulfilled if  $\Sigma$  is small. However, whenever  $\sigma$  is finite,  $\Sigma$  can only be zero for vanishing slopes of  $\bar{A}$ , i.e.,  $\partial\bar{A}/\partial\bar{E} = 0$ . Therefore, for finite  $\sigma$ , the ETH is fulfilled if  $\Sigma \rightarrow \partial\bar{A}/\partial\bar{E}\sigma$  in the limit of large system sizes [21].

A crucial point in this paper is of course finite-size scaling. To render this scaling as convincing as possible, one needs data on systems as large as possible. Usually, checking the ETH requires exact diagonalization [24, 25] that is limited to rather small system sizes. Thus, we employ a recently suggested method [21] that is based on dynamical typicality and allows for the extraction of

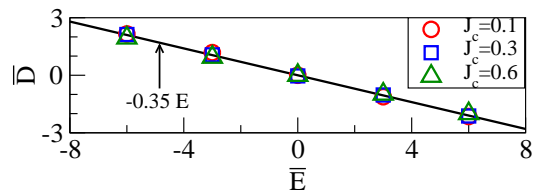


FIG. 2: (color online) Mean energy difference  $\bar{D}$  of energy eigenstates in an energy shell of width  $\sigma = 0.6$  around  $\bar{E}$ , calculated for the model in Fig. 1 (a) with anisotropy  $\Delta = 0.3$  and system size  $N_L = 8$ . For the “average eigenstate”, the distribution of energy onto the subsystems is proportional to their sizes.

information on the ETH from the temporal propagation of pure states. This propagation can be performed by iterative algorithms such as Runge-Kutta [20–22], Chebyshev [32, 33], etc. and is feasible for larger system sizes. We use a fourth-order Runge-Kutta iterator with a sufficiently small time step. Due to typicality-related reasons, the so-computed quantities  $\bar{A}$  and  $\Sigma$  are subject to statistical errors. These errors, however, turn out to be smaller than the symbol sizes used in this paper [22].

We study systems consisting of two weakly coupled XXZ spin-1/2 chains (except for one example discussed below). The Hamiltonian of the chains has open boundary conditions and is given by

$$H_j = J \sum_{i=1}^{N_j-1} (S_{i,j}^x S_{i+1,j}^x + S_{i,j}^y S_{i+1,j}^y + \Delta S_{i,j}^z S_{i+1,j}^z) + \sum_i^{N_j} h_{i,j} S_{i,j}^z, \quad (4)$$

where  $j = L, R$  labels the “left” and “right” chain.  $N_L, N_R$  are the respective numbers of spins in the chains, see Figs. 1 (a)-(c).  $J = 1$  is the antiferromagnetic exchange coupling constant and  $\Delta$  is the exchange anisotropy.  $h_{i,j}$  are spatially random magnetic fields in  $z$  direction that are drawn at random according to a uniform distribution between  $-W/2$  and  $W/2$ . This way of introducing disorder is similar to the random on-site potential of the Anderson model, widely investigated in the context of many-body localization [34].

To allow for energy exchange, we add a coupling term  $H_C$  between the two chains:  $H = H_L + H_R + H_C$ . This term has a very similar form and reads

$$H_C = J_C \sum_{i=1}^{N_L} c_i (S_{i,L}^x S_{i,R}^x + S_{i,L}^y S_{i,R}^y + \Delta S_{i,L}^z S_{i,R}^z), \quad (5)$$

where  $J_C$  is the coupling strength. For  $c_i = 1$ , the total Hamiltonian  $H$  represents a nonintegrable structure of ladder type while, for  $c_i = \delta(i, 1)$ ,  $H$  reduces to a single chain. This chain is integrable for  $J = J_C$  and  $W = 0$  only. We also consider the intermediate case with  $c_i = \delta(i, 1) + \delta(i, N_L)$  and a two-dimensional situation with

$c_i = 1$ : In this situation the chains in Eq. (4) are replaced by  $N_j \times N_j$  lattices with interactions between all nearest neighbors and the coupling in Eq. (5) is replaced by an interaction at the contact of the lattices, as illustrated in Fig. 1 (d).

The observable  $A$  we are going to investigate for accord with the ETH is the energy difference.  $A$  is represented by the operator  $D = H_L - H_R$ . For any left-right symmetric model and observable, the ETH is necessarily fulfilled. Thus, to avoid this trivial case, we choose right chains to consist of twice as much spins as the left chains throughout this paper, see Figs. 1 (a)-(c). In the two-dimensional situation we choose the right-lattice side to have one spin more than the left-lattice side.

### III. RESULTS ON NONINTEGRABLE SYSTEMS

First, we consider  $\bar{D}(\bar{E})$ , i.e., the mean energy difference for the energy eigenstates in a small energy interval centered at  $\bar{E}$ . We control the smallness of this energy interval by choosing  $\sigma = 0.6$ . (This choice is kept for the remainder of this paper.) Results on the model in Fig. 1 (a) are displayed in Fig. 2 for various coupling strengths  $J_C$  at fixed anisotropy  $\Delta = 0.3$  and system size  $N_L = 8$ .

To gain insight into the results in Fig. 2, let us consider the following analog to the standard equipartition theorem: Assume that every term in the Hamiltonian (“bond”) contains for energy eigenstates an amount of energy proportional to its strength. For weak coupling, the energies corresponding to terms of  $H_C$  can be neglected. Then one expects a left/right-chain partition of energy as  $(N_L - 1)/(N_R - 1) = 7/15$ , yielding an energy difference  $\bar{D} = (N_L - N_R)/(N_R + N_L - 2) \bar{E} = -4\bar{E}/11$ . This expectation is indicated by the solid line in Fig. 2. Clearly, the equipartition assumption is well justified for a wide range of interactions strengths  $J_C \leq 0.6$ . We find this principle to hold for each model addressed in this paper, even though not shown explicitly here. This finding is a first main result, although not at the center of the investigation in this paper.

Next we turn to the ETH. To limit computational effort, we focus on the energy regime around  $\bar{E} = 0$ , however, we have found similar results for other points in energy space. For the  $E = 0$  regime we compute both,  $d_{\text{eff}} = \text{Tr}\{e^{-(H-\bar{E})^2/2\sigma^2}\}$  and  $\Sigma' = \Sigma - \partial\bar{D}/\partial\bar{E}\sigma$ .  $d_{\text{eff}}$  has the meaning of the number of eigenstates that constitute the “relevant” energy shell.  $\Sigma'$  is the quantity that is expected to approach zero if the ETH is fulfilled. (We get  $\partial\bar{D}/\partial\bar{E}\sigma = 0.21$  throughout this paper.) For all models studied, we show in Fig. 3 a double logarithmic plot of  $\Sigma'$  as a function of  $d_{\text{eff}}$  that increases with system size.

In Figs. 3 (a)-(c) we summarize our results on  $\Sigma'$  for the model in Fig. 1 (a): In Fig. 3 (a) we vary the coupling strength  $J_C$  at fixed anisotropy  $\Delta = 0.3$ ; In Fig. 3 (b) we vary the anisotropy  $\Delta$  at fixed coupling strength  $J_C = 0.3$ ; and in Fig. 3 (c) we study cases of weak and in-

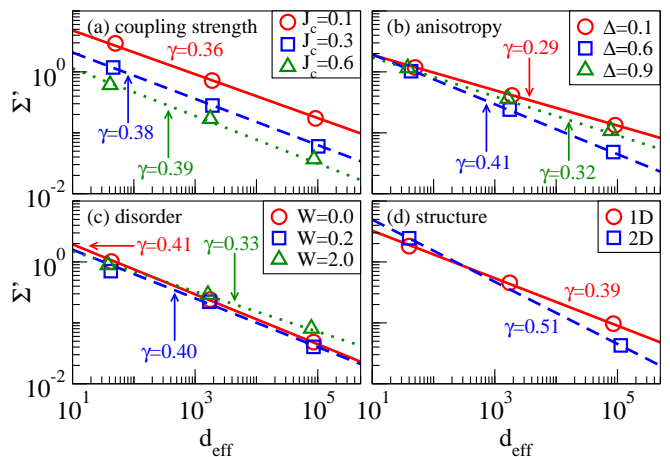


FIG. 3: (color online) The parameter  $\Sigma'$ , quantifying the degree of ETH violation, as a function of the effective dimension  $d_{\text{eff}}$  that increases with system sizes. The violation appears to vanish according to a power law in the limit of large system sizes, regardless of the properties of the specific models studied in (a)-(d). For model parameters, see text.

intermediate amount of disorder for  $\Delta = 0.6$  and  $J_C = 0.3$ . In Fig. 3 (d) we show results for the same values  $\Delta = 0.6$  and  $J_C = 0.3$  but for  $W = 0$  and the different coupling structure in Fig. 1 (b) and the two-dimensional case in Fig. 1 (d).

In all cases,  $\Sigma'$  apparently scales with  $d_{\text{eff}}$  as a power law  $\Sigma' \propto d_{\text{eff}}^{-\gamma}$ , which is in accord with the findings in Ref. [25]. Consequently, the ETH is fulfilled in the limit of large system sizes. This is our second main result. It indeed indicates that the relaxation of the energy difference between weakly coupled quantum objects may be generically expected for all sorts of initial states. For a random-matrix model, one would expect a power-law scaling with the exponent  $\gamma = 0.5$ . For all nonintegrable cases we studied we find a slightly different exponent. If we call closeness to  $\gamma = 0.5$  the “amount” of nonintegrability, then the two-dimensional case in Fig. 1 (d) is the most nonintegrable one studied here. For the one-dimensional cases, the amount of nonintegrability does not depend crucially on the coupling constant  $J_C$  in the small  $J_C$  regime, while the dependence on the anisotropy  $\Delta$  is nonmonotonic.

### IV. MICROCANONICAL OBSERVABLE, DISPLACED STATES AND RESULTS ON INTEGRABLE SYSTEMS

The above findings certainly raise immediately the question of ISI equilibration in integrable models: Is it reasonable to expect the violation of ISI equilibration for two subsystems which are connected to form an integrable system? Comparable investigations found answers in both directions [27, 28, 35], even for nonintegrable systems [14, 15, 36]. To analyze this question, we study a

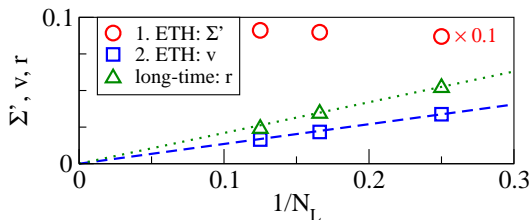


FIG. 4: (color online) The ETH parameter  $\Sigma'$  (circles), the scaled ETH parameter  $v$  (squares), and the long-time value  $r$  for the integrable Heisenberg chain in an energy window of width  $\sigma = 0.6$  around energy  $\bar{E} = 0$ . All quantities are shown as a function of the inverse number of spins  $1/N_L$ .

pure Heisenberg chain, from the point of view depicted in Fig. 1 (c). As already mentioned, this Heisenberg chain is integrable for  $J_C = 1$ ,  $\Delta = 0.6$  and  $W = 0$ . For this model, we show in Fig. 4 (circles) results on  $\Sigma'$  as a function of  $1/N_L$ .

Unlike all previous examples,  $\Sigma'$  does not decrease as system size increases, which is in accord with the system being integrable. To clarify the impact on relaxation, we analyze the dynamics of “microcanonical” and “observable-displaced” initial states  $\rho_{\text{MOD}}$ ,

$$\rho_{\text{MOD}} \propto e^{-(H^2 + \beta^2 [D - d(0)]^2) / 2\sigma^2}. \quad (6)$$

Obviously, the parameter  $d(0)$  controls the degree of observable displacement. The energy is concentrated within a width  $\sigma$  around zero. Since  $H$  and  $D$  do not commute, we need to find a compromise between energy concentration and observable displacement, done by tuning  $\beta$ . We choose  $\sigma = 0.6$ ,  $\beta = 0.5$ , and  $d(0) = \pm N_L$ . This state may be viewed as being based on Jayne’s principle: It represents the maximum-entropy state under given means and variances for energy and observable.

A comment on the usage of this type of initial states as opposed to initial states generated by quantum quenches may be instructive. While quantum-quench approaches produce a complex, non-stationary state, it may or may not make the considered observable deviating from its long-time average. The MOD state, on the other hand, is deliberately designed to obtain a specific initial value of the considered observable while keeping the energy reasonably well-defined. Thus, the MOD approach facilitates the generation of initial values of the observable that are “substantially off-equilibrium”, to put it in a catchy phrase. Using the above parameters, we indeed get  $\text{Tr}\{\rho_{\text{MOD}} D(0)\} \approx d(0) = \pm N_L$ . The largest eigenvalue of  $D$  is upper-bounded by  $D \leq 9/4(N_L - 1)$ . Hence, the initial expectation value of  $D$  reaches at least 50% of the difference between its highest possible value and its long-time average. Corresponding values for standard quench dynamics are usually much lower [15, 16].

Note also that such a MOD state does not necessarily feature a smooth probability distribution w.r.t. energy, as suggested in Ref. [37] to explain ISI.

Numerically,  $\rho_{\text{MOD}}$  is challenging to compute for sys-

tems beyond the reach of exact diagonalization. Thus, we prepare the partially random state

$$|\phi_{\text{MOD}}\rangle = \langle\varphi|\rho_{\text{MOD}}|\varphi\rangle^{-1/2} \rho_{\text{MOD}}^{1/2} |\varphi\rangle, \quad (7)$$

where  $|\varphi\rangle$  is a random state drawn according to the unitary invariant (Haar-) measure. In the context of typicality, e.g. from Ref. [19, 22], it may be inferred that the dynamics of  $|\phi_{\text{MOD}}\rangle$  are similar to those of  $\rho_{\text{MOD}}$  w.r.t. to the observable, i.e.,

$$d(t) = \langle\phi_{\text{MOD}}|D(t)|\phi_{\text{MOD}}\rangle = \text{Tr}\{\rho_{\text{MOD}} D(t)\} + \epsilon, \quad (8)$$

where  $\epsilon$  is a random variable with zero mean. The standard deviation of  $\epsilon$  is upper bounded by  $(\text{Tr}\{\rho_{\text{MOD}} D^4\}/d_{\text{eff}})^{1/2}$ . Thus, since the density of states is large at  $\bar{E} = 0$ , we get  $\epsilon \approx 0$ .

Using Runge-Kutta we can prepare these initial states and compute the time evolution of energy-difference expectations  $d(t)$  divided by their initial values  $d(0)$ , i.e.,  $r(t) = d(t)/d(0)$ . In Fig. 5 we depict our results for three system sizes  $N_L = 4, 6$  and  $8$ . Remarkably, the scaled differences  $r(t)$  are practically independent of the sign of the initial value  $d(0)$ . While the energy difference  $r(t)$  decays, it does not decay all the way to zero. In fact, the fluctuations around the corresponding nonzero equilibrium value decrease for increasing system size  $N_L$ . Thus, for finite systems, there is indeed no clean ISI equilibration. Since we find the same behavior for the overwhelming majority of all states prepared according to Eq. (7), it is reasonable to claim that the validity of the ETH is imperative for ISI equilibration. However, comparing Figs. 5 (a), (b), and (c) indicates that  $r(t)$  decreases at large times as system size increases. (Considering  $r(t)$  at large times as a central quantity is also suggested in Ref. [38].) This finding implies that ISI equilibration may be expected for this specific system and observable in the limit of large system sizes, regardless of the ETH being fulfilled. While it is well-known that also integrable systems may exhibit ISI (see the corresponding statement at the beginning of this section), these examples either refer to situations where the ETH may apply w.r.t. the considered observable regardless of integrability [14] and/or initial states generated from quenches that are not tailored to make the considered observable initially deviating largely from its long-time average [15]. In contrast to that, our finding addresses the occurrence of ISI for a situation where the violation of the ETH is numerically evident and the initial state is specifically chosen to initially deviate largely from its long-time average. This is a third main result of our paper.

The above results naturally lead to the question why larger systems exhibit equilibration that is closer to ISI even though  $\Sigma'$  is essentially the same for large and small systems. To clarify this question, let us consider a quantity that takes the “natural” scale of the operator into account, rather than just the bare  $\Sigma'$ . Therefore, we define a scaled ETH parameter  $v$  as  $v := (\Sigma')^2/\delta^2$ , where  $\delta$  is the variance of the operator spectrum within the respective energy regime, i.e.,  $\delta^2 = \bar{D}^2 - \bar{D}^2$ . The bar in  $\bar{D}^2$  and

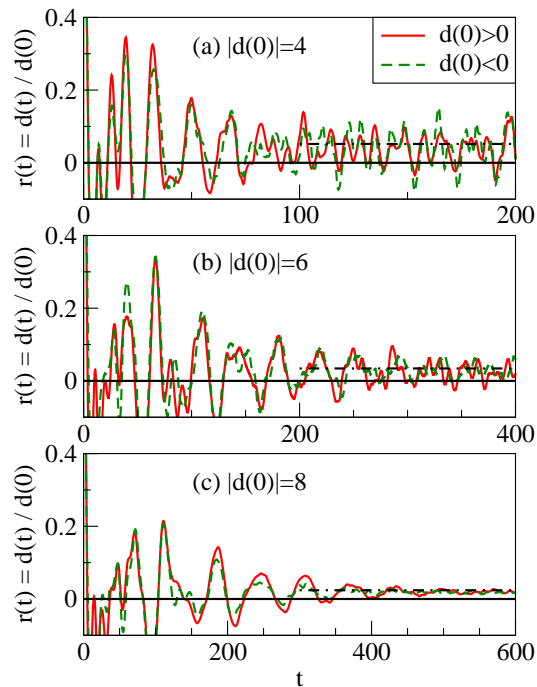


FIG. 5: Real-time decay of energy-difference expectation values  $d(t)$ , divided by their initial values  $d(0)$ , for initial states in Eq. (7) and three system sizes: (a)  $N_L = 4$ , (b)  $N_L = 6$ , and (c)  $N_L = 8$ . While  $r(t) = d(t)/d(0)$  does not vanish for long times and finite systems, comparing (a), (b), and (c) indicates a vanishing  $r(t)$  for long times in the limit of large system sizes. For more details on finite-size scaling, see Fig. 4 (triangles).

$\overline{D}$  is still defined according to Eq. (3). Obviously, even if  $\Sigma'$  does not decrease as system size increases,  $v$  may still do so. To find out whether or not it actually does, one has to compute the two quantities  $\overline{D^2}$  and  $\overline{D}$ . This computation can be done by the same typicality-based method used so far in this paper. In Fig. 4 (squares) we show the corresponding result. Apparently,  $v$  vanishes in the limit of large system sizes even though  $\Sigma'$  does not. This observation suggests that  $v$  is a reliable predictor of ISI equilibration that can vanish even if systems are integrable or close to integrability.

## V. SUMMARY AND CONCLUSION

In this paper we studied the validity of the ETH and its role for the occurrence of ISI equilibration in closed quantum many-body systems. Using the concept of dynamical typicality, we presented an extensive numerical analysis of energy exchange in integrable and nonintegrable spin-1/2 systems of large size outside the range of exact diagonalization. In case of nonintegrable systems, our finite-size scaling showed that the ETH becomes valid in the thermodynamic limit and can serve as the underlying mechanism for ISI equilibration. In case of integrable systems, however, indication of ISI equilibration has been observed despite the violation of the ETH and initial states that specifically facilitate the deviation of the observable from its equilibrium value. We established a connection between this observation and the need of choosing a proper parameter within the ETH.

- 
- [1] S. Trotzky, P. Cheinet, S. Folling, M. Feld, U. Schnorrberger, A. M. Rey, A. Polkovnikov, E. A. Demler, M. D. Lukin, and I. Bloch, *Science* **319**, 295 (2008).
- [2] S. Hofferberth, I. Lesanovsky, B. Fischer, T. Schumm, and J. Schmiedmayer, *Nature* **449**, 324 (2007).
- [3] I. Bloch, J. Dalibard, and W. Zwerger, *Rev. Mod. Phys.* **80**, 885 (2008).
- [4] M. Cheneau, B. Barmettler, D. Poletti, M. Endres, P. Schauß, T. Fukuhara, C. Gross, I. Bloch, C. Kollath, and S. Kuhr, *Nature* **481**, 484 (2012).
- [5] T. Langen, R. Geiger, M. Kuhnert, B. Rauer, and J. Schmiedmayer, *Nature Phys.* **9**, 640 (2013).
- [6] O. Lyckovskiy, *Phys. Rev. E* **82**, 011123 (2010).
- [7] N. Linden, S. Popescu, A. J. Short, and A. Winter, *Phys. Rev. E* **79**, 061103 (2009).
- [8] J. M. Deutsch, *Phys. Rev. A* **43**, 2046 (1991).
- [9] M. Srednicki, *Phys. Rev. E* **50**, 888 (1994).
- [10] M. Rigol, V. Dunjko, and M. Olshanii, *Nature* **452**, 854 (2008).
- [11] P. Reimann, *Phys. Rev. Lett.* **101**, 190403 (2008).
- [12] A. del Campo, *Phys. Rev. A* **84**, 012113 (2011).
- [13] A. Riera, C. Gogolin, and J. Eisert, *Phys. Rev. Lett.* **108**, 080402 (2012).
- [14] D. Rossini, A. Silva, G. Mussardo, and G. E. Santoro, *Phys. Rev. Lett.* **102**, 127204 (2009).
- [15] M. Rigol, M. Srednicki, *Phys. Rev. Lett.* **108**, 110601 (2012).
- [16] M. Rigol, *Phys. Rev. Lett.* **103**, 100403 (2009).
- [17] G. Biroli, C. Kollath, and A. M. Läuchli, *Phys. Rev. Lett.* **105**, 250401 (2010).
- [18] S. Goldstein, J. L. Lebowitz, R. Tumulka, and N. Zanghi, *Phys. Rev. Lett.* **96**, 050403 (2006).
- [19] C. Bartsch and J. Gemmer, *Phys. Rev. Lett.* **102**, 110403 (2009).
- [20] T. A. Elsayed and B. V. Fine, *Phys. Rev. Lett.* **110**, 070404 (2013).
- [21] R. Steinigeweg, A. Khodja, H. Niemeyer, C. Gogolin, and J. Gemmer, *Phys. Rev. Lett.* **112**, 130403 (2014).
- [22] R. Steinigeweg, J. Gemmer, and W. Brenig, *Phys. Rev. Lett.* **112**, 120601 (2014).
- [23] T. N. Ikeda, Y. Watanabe, and M. Ueda, *Phys. Rev. E* **87**, 012125 (2013).
- [24] R. Steinigeweg, J. Herbrych, and P. Prelovšek, *Phys. Rev. E* **87**, 012118 (2013).
- [25] W. Beugeling, R. Moessner, and M. Haque, *Phys. Rev. E* **89**, 042112 (2014).
- [26] M. Rigol, A. Muramatsu, and M. Olshanii, *Phys. Rev. A* **74**, 053616 (2006).

- [27] M. Rigol, V. Dunjko, V. Yurovsky, and M. Olshanii, Phys. Rev. Lett. **98**, 050405 (2007).
- [28] L. F. Santos, F. Borgonovi, and F. M. Izrailev, Phys. Rev. Lett. **108**, 094102 (2012).
- [29] K. He and M. Rigol, Phys. Rev. A **87**, 043615 (2013).
- [30] I. Gudyma, A. Maksymov, and M. Dimian, Phys. Rev. E **88**, 042111 (2013).
- [31] T. Monnai, Phys. Rev. E **84**, 011126 (2011).
- [32] H. De Raedt and K. Michielsen, *Computational Methods for Simulating Quantum Computers* in *Handbook of Theoretical and Computational Nanotechnology* (American Scientific Publishers, Los Angeles, 2006).
- [33] K. De Raedt, K. Michielsen, H. De Raedt, B. Trieu, G. Arnold, M. Richter, T. Lippert, H. Watanabe, and N. Ito, Comput. Phys. Commun. **176**, 121 (2007).
- [34] A. Pal and D. A. Huse, Phys. Rev. B **82**, 174411 (2010).
- [35] T. Kinoshita, T. Wenger, and D. S. Weiss, Nature **440**, 900 (2006).
- [36] C. Gogolin, M. P. Müller, and J. Eisert, Phys. Rev. Lett. **106**, 040401 (2011).
- [37] T. N. Ikeda, Y. Watanabe, and M. Ueda, Phys. Rev. E **84**, 021130 (2011).
- [38] V. A. Yurovsky and M. Olshanii, Phys. Rev. Lett. **106**, 025303 (2011).